Quantum dynamics of charge transfer on the one-dimensional lattice: Wave packet spreading and recurrence

V N Likhachev, O I Shevaleevskii, and G A Vinogradov[†]

Emanuel Institute of Biochemical Physics, Russian Academy of Sciences, Moscow, Russian Federation

(Received 1 April 2015; revised manuscript received 27 August 2015; published online 30 November 2015)

The wave function temporal evolution on the one-dimensional (1D) lattice is considered in the tight-binding approximation. The lattice consists of N equal sites and one impurity site (donor). The donor differs from other lattice sites by the on-site electron energy E and the intersite coupling C. The moving wave packet is formed from the wave function initially localized on the donor. The exact solution for the wave packet velocity and the shape is derived at different values E and C. The velocity has the maximal possible group velocity $v = 2$. The wave packet width grows with time $\sim t^{1/3}$ and its amplitude decreases $\sim t^{-1/3}$. The wave packet reflects multiply from the lattice ends. Analytical expressions for the wave packet front propagation and recurrence are in good agreement with numeric simulations.

Keywords: quantum dynamics, tight-binding approximation, charge transport

PACS: 87.15.–v, 42.15.Dp **DOI:** 10.1088/1674-1056/25/1/018708

1. Introduction

Charge transfer (CT) is the key event in many processes in living and inorganic matter; photosynthesis, breathing and many others are the well known examples in living matter.[1–6] Very efficient CT was found later in synthetics analogous of DNA and polypeptides.[7–11] These substances have well organized structures consisting of repeating units, DNA bases (usually adenine) or peptide groups, and represent very good models for CT in one-dimensional systems.

The tight-binding approximation (TBA) is an efficient tool to study the CT. This approach is dated back to the Slater–Koster paper.[12] The TBA single-particle Hamiltonian can be written as $\boldsymbol{H} = \sum_{\langle i,j\rangle} \xi_{i,j}\,|i\rangle\langle j| + \sum_i \varepsilon_i |i\rangle\langle i|$, where $\xi_{i,j}$ is the intersite coupling between i-th and j-th sites (known also as the "hopping integral"), ε_i is the on-site energy on the i-th site. The wave function is constructed as the superposition of wave functions for isolated sites.

Many efforts were undertaken to study the wave function evolution using the TBA approximation. One well investigated example is the TBA on the disordered lattice. The case of the static disorder, when on-site energies take random values, received special attention. The Anderson localization[13] was studied extensively employing the TBA Hamiltonian.[14–18]

Two models of random values distribution are studied most often. In the first model, random on-site energies ε_i are chosen uniformly from the interval $[-W/2, W/2]$, with W denoting the disorder strength.[19,20] Random values in the second model are determined as $\varepsilon_i = \lambda\cos(2\pi i\sigma + \phi)$. On-site energies are random values if σ is incommensurate with the lattice period.[21,22]

It has been known that if the disorder strength is moderately small, then the moving wave packets are formed from the initially localized wave function. This moving wave function pulse can transport the charge. In studies of the wave packet dynamics it was found that the wave packet initially moves ballistically $\sim t$, but at large times the wave packet movement is diffuse $\sim t^{\beta}$ with β taking a wide range of values.[23,24] By virtue of problems associated with the investigations of random lattices, most of the studies were performed by approximate methods or numerically.

In the present paper, we consider the problem of the wave function temporal evolution. The TBA approximation is utilized. The lattice is homogeneous, i.e., both types of disorder–diagonal and off-diagonal, are absent. The wave function is initially localized on one site, i.e., $\psi_j(t=0) = \delta_{j,1}$. The formed moving wave packet can multiply reflect from the ends of the lattice. It should be remembered that the recurrence phenomena to the initial state are in general well known. The Fermi–Pasta–Ulam recurrence is an example of nonlinear classical dynamics.[25,26] The other example is the interaction of the isolated vibrational mode with the continuous spectrum.[27]

The recurrence in quantum systems was considered by Zwanzig[28] for the discrete equidistant spectrum where a single level is initially occupied. The analysis of the Zwanzig's problem was performed for the resonance[29] and for the non-resonance[30] cases.

There is a further point to be outlined. The considered TBA model can also govern the evolution of vibrational excitations. The vibrational energy transport in molecular wires was considered by Benserskii and coauthors.[31,32] The recurrence phenomena (Loschmidt echo) in molecular chains and

[†]Corresponding author. E-mail: gvin@deom.chph.ras.ru

© 2016 Chinese Physical Society and IOP Publishing Ltd

nanoparticles was also analyzed.[29]

In the present paper we thoroughly analyze the simplest case of the defect-free lattice. Nevertheless the considered model can be relevant to systems with defects if the disorder strength is not too large. It is known for the three-dimensional lattices, that the critical value W, below which the system is conductive, is rather large, $W_{\rm cr} \approx 8.59 \pm 0.05$.[33]

It worth mentioning that Anderson's localization theorem[13] is, strictly speaking, valid for one-dimensional systems in the thermodynamical limit ($N \to \infty$). The situation differs for the final-sized systems. There is the scaling which relates the parameters N and $W_{\rm cr}$.[33–38] But $W_{\rm cr}$ does not depend on N in one-dimensional systems and, according to our preliminary results, lies in the region $W_{\rm cr} \approx 2$. It means that if the diagonal disorder strength $W \lesssim 2$ then results obtained for the defect-free lattice can be applicable to systems with defects.

If defects are off-diagonal, e.g., due to thermal fluctuations, then the above mentioned arguments are also valid. The defect-free approximation is fulfilled if the temperature is not too high ($kT/2$ in one-dimensional systems should be compared with a critical value $W_{\rm cr}$).

Exact expressions are also derived for the wave packet shape and velocity at arbitrary time instants including the wave packet parameters after reflections. This is done for the most interesting case when the wave function is initially totally localized on the lattice end which plays the role of an electron donor in experiments on the charge transfer in DNA.[8,9]

The "electron ping–pong" was found experimentally in DNA,[39] when a charge is triggered consecutively within the same DNA duplex after a charge injection. This phenomenon is also considered and analytical expressions for the wavefunction amplitude on the electron donor are derived.

The considered problem is relevant to the charge transport and our results mimic to some degree the numerous experiments on charge transfer in low-dimensional systems. Because the wave function evolution is governed by the quantum mechanics laws, the problem under consideration is designated as the quantum dynamics of charge transfer.

2. Setting up a problem

We consider the lattice consisting of $(N+1)$ sites. The left-most site is the "electron donor". The wave function is initially totally localized on this site. Other N sites are a "reservoir" through which the wave function spreads.

In the second quantization representation, the TBA Hamiltonian is of the form

$$\boldsymbol{H} = Ea^+a^- + C\left(a^+b_1^- + b_1^+a^-\right) + \sum_{j=1}^{N} \varepsilon_j b_j^+ b_j^- + \sum_{j=1}^{N-1} \xi_{j+1,j} b_{j+1}^+ b_j^- + \sum_{j=2}^{N} \xi_{j-1,j} b_{j-1}^+ b_j^- , \quad (1)$$

where $a^{+/-}$ is the creation/annihilation operator on the donor; $b_j^{+/-}$ – analogous for j-th site in the reservoir ($j = 1, 2, \ldots, N$), E is the on-site energy on the donor, C is the intersite coupling between the donor and the first site of the reservoir, $\xi_{j-1,j}$ is the intersite coupling for the nearest neighbor sites in the reservoir, and ε_j is on-site energy on the j-th lattice site.

We consider a simple model when all on-site energies of the reservoir are equal and $\varepsilon_j = \text{const} = 0$, which corresponds to the choice of the reference point for the electron energy. All intersite couplings on the lattice $\xi_{j-1,j} = 1$, which corresponds to the choice of the energy unit. In general, $E \neq 0$ and $C \neq 1$ for the coupling between the donor and the reservoir.

It is instructive to rewrite the Hamiltonian (1) in the matrix representation for the sake of convenience

$$\boldsymbol{H} = \begin{pmatrix} E & C & 0 & \cdots & 0 & 0 \\ C & \mathbf{0} & \mathbf{1} & \cdots & \mathbf{0} & \mathbf{0} \\ 0 & \mathbf{1} & \mathbf{0} & \cdots & \mathbf{0} & \mathbf{0} \\ \vdots & \vdots & \vdots & \ddots & \vdots & \vdots \\ 0 & \mathbf{0} & \mathbf{0} & \cdots & \mathbf{0} & \mathbf{1} \\ 0 & \mathbf{0} & \mathbf{0} & \cdots & \mathbf{1} & \mathbf{0} \end{pmatrix}. \quad (2)$$

Matrix elements related to the reservoir are highlighted in bold. The discrete wave function is the $(N+1)$-vector

$$\boldsymbol{\Psi}(t) = a(t), b_1(t), b_2(t), \ldots, b_N(t), \quad (3)$$

where $a(t)$ is the wave function amplitude on the donor and $b_j(t)$ ($j = 1, 2, \ldots, N$) are amplitudes on reservoir sites.

The problem is to find how the electronic populations on all sites change in time. The dimensionless ($\hbar = 1$) Schrödinger equations for the wave function evolution have the form

$$\begin{aligned} \mathrm{i}\dot{a}(t) &= Ea(t) + Cb_1(t), \\ \mathrm{i}\dot{b}_1(t) &= b_2(t) + Ca(t), \\ \mathrm{i}\dot{b}_2(t) &= b_1(t) + b_3(t), \\ &\cdots \\ \mathrm{i}\dot{b}_N(t) &= b_{N-1}(t), \end{aligned} \quad (4)$$

with the initial conditions $a(t=0) = 1$ and $b_j(t=0) = 0$ ($j = 1, 2, \ldots, N$). Dots over $a(t)$ and $b_j(t)$ mean the time derivatives. The characteristic quantum time unit $\sim \hbar/\langle\xi\rangle$ and $\langle\xi\rangle$ is the typical value of the intersite coupling energy ($\langle\xi\rangle = 1$ in Eq. (4)). The length unit is the lattice period.

If Eq. (4) is integrated numerically then the phenomenon of recurrence, i.e., multiple returning to the initial state, is observed (the electronic "ping-pong" was found experimentally[39]). The result is shown in Fig. 1.

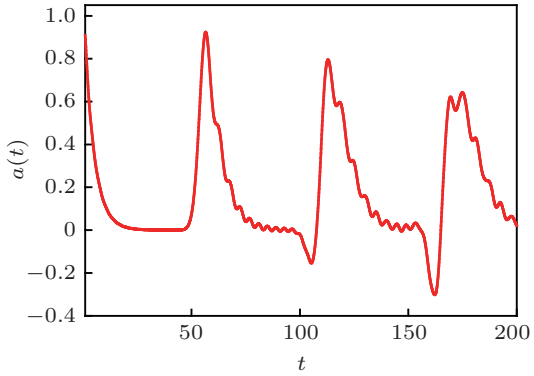


Fig. 1. (color online) The dependence of the wave function amplitude $a(t)$ on the donor versus time. The wave function returns many times (three times in the figure) to the donor with a slightly decreasing amplitude. Parameters: $E=0$, $C=\sqrt{2}$, $N=50$.

The goal of the present paper is to consider the wave packet spreading through the lattice and its reflections from the lattice ends. The quantum dynamical problem of the wave function evolution can be considered as the interaction of the donor with the reservoir. It is solved using the expansion in terms of the eigenfunctions of the reservoir. The reservoir is represented by the $N\times N$ tridiagonal matrix with zero leading diagonal and the unity values on the secondary diagonals (highlighted in bold in Eq. (2)). Eigenvalues $\varepsilon(k)$ and eigenfunctions $q_j(k)$ of this matrix are well known as

$$\varepsilon(k)=2\cos\left(\frac{\pi k}{N+1}\right),$$
$$q_j(k)=\sqrt{\frac{2}{N+1}}\sin\left(\frac{\pi kj}{N+1}\right). \tag{5}$$

It is convenient to consider the problem in terms of amplitudes of modes $b(k)$ instead of amplitudes on the lattice sites b_j. These values are related by the orthogonal relationship

$$b(k,t)\equiv\sum_{j=1}^{N}q_j(k)\,b_j(t),\quad b_j(t)\equiv\sum_{k=1}^{N}q_j(k)\,b(k,t), \tag{6}$$

and then, system (4) can be rewritten in the form

$$\begin{aligned}\mathrm{i}\dot{a}(t) &= Ea(t)+C\sum_{k=1}^{N}q_1(k)b(k,t),\\ \mathrm{i}\dot{b}(k,t) &= \varepsilon(k)b(k,t)+Ca(t)q_1(k),\quad k=1,2,\ldots,N.\end{aligned} \tag{7}$$

Amplitudes $b(k,t)$ in Eq. (7) can be expressed through amplitude $a(t)$

$$b(k,t)=q_1(k)\exp[-\mathrm{i}\,\varepsilon(k)t]\int_0^t a(\tau)\exp[\mathrm{i}\,\varepsilon(k)\,\tau]\,\mathrm{d}\tau. \tag{8}$$

Substituting this expression into Eq. (7) for $a(t)$, one can get the integro-differential equation for the amplitude $a(t)$ on the donor

$$\dot{a}(t)=-\mathrm{i}E\,a(t)-C^2\int_0^t B^N(t-\tau)\,a(\tau)\,\mathrm{d}\tau, \tag{9}$$

where the kernel $B^N(t)$ is given by the following sum:

$$B^N(t)=\frac{2}{N+1}\sum_{k=1}^{N}\sin^2\left(\frac{\pi k}{N+1}\right)\times\exp\left[-2\mathrm{i}\cos\left(\frac{\pi k}{N+1}\right)t\right]. \tag{10}$$

In the next section, we solve Eq. (9) for the amplitude $a(t)$ on the donor and then discuss the formation of a wave packet pulse at time less than the time of the first reflection from the right end of the lattice.

3. The decay of the initial state $a(t=0)=1$ in the semi-infinite lattice

Initially, we consider the decay kinetics of the initial state $a(t=0)=1$ in the semi-infinite lattice ($N\to\infty$). The amplitude on the donor is labelled by $a_0(t)$ in this case. The limit $N\to\infty$ for the kernel $B^N(t)$ is also used. The expression for $B^N(t)$ is denoted by $B_0(t)$ at $N\to\infty$. In this limit, equation (10) transforms to the integral with the solution[40]

$$B_0(t)\equiv\lim_{N\to\infty}B^N(t)=\mathrm{J}_0(2t)+\mathrm{J}_2(2t), \tag{11}$$

where J_0 and J_2 are Bessel functions of corresponding orders. Then one gets the following equation for the amplitude $a_0(t)$:

$$\dot{a}_0(t)=-\mathrm{i}Ea_0(t)-C^2\int_0^t B_0(t-\tau)\,a_0(\tau)\,\mathrm{d}\tau. \tag{12}$$

This first-order differential equation can be solved using the Laplace transformation

$$a_0(p)=\frac{1}{p+\mathrm{i}E+C^2B_0(p)}, \tag{13}$$

where the Laplace transform $B_0(p)$ of the function $B_0(t)$[40]

$$B_0(p)=\frac{1}{2}\left(\sqrt{p^2+4}-p\right). \tag{14}$$

The amplitude $a_0(t)$ can be obtained by the inverse Laplace transformation

$$a_0(t)=\int_{d-\mathrm{i}\infty}^{d+\mathrm{i}\infty}\frac{\exp(pt)}{p+\mathrm{i}E+\dfrac{C^2}{2}\left(\sqrt{p^2+4}-p\right)}\,\mathrm{d}p,\quad d>0. \tag{15}$$

This form of $a_0(t)$ is very inconvenient for both the analysis and numerical computations (integral with the upper infinite limit converges very slowly). This integral obtains a more convenient form if the integration contour is closed around the cut $[-2\mathrm{i},+2\mathrm{i}]$. If this takes place, the square root $\sqrt{p^2+4}$ must be represented as $-\mathrm{i}\sqrt{\mathrm{i}p+2}\,\sqrt{\mathrm{i}p-2}$. The integration contour can be closed if amplitude $a_0(p)$ has no poles. Assuming that poles are absent, closing the integration contour and summing the integrals along both sides of the cut, one gets the following expression for the amplitude $a_0(t)$:

$$a_0(t)=\frac{1}{\pi}\int_{-2}^{+2}\exp(\mathrm{i}\,\omega t)$$

$$\times \mathrm{Im}\left[\omega + E - \frac{C^2}{2}\left(\omega + \mathrm{i}\sqrt{4-\omega^2}\right)\right]^{-1} \mathrm{d}\omega. \quad (16)$$

Few special cases can be noted, when the integral (16) is calculated explicitly and the amplitude $a_0(t)$ is expressed in terms of Bessel functions[40]

$$\begin{aligned} a_0(t) &= \mathrm{J}_0(2t), \quad (E=0,\, C=\sqrt{2}), \\ a_0(t) &= \mathrm{J}_0(2t) + \mathrm{J}_2(2t), \quad (E=0,\, C=1), \\ a_0(t) &= \mathrm{J}_0(2t) - \mathrm{i}\mathrm{J}_1(2t), \quad (E=1,\, C=1). \end{aligned} \quad (17)$$

An integro-differential equation for the amplitude $a_0(t)$ is additionally derived in Appendix A, and its solution is obtained as a series of Bessel functions. The series is rather cumbersome, but expressions take simple forms in several particular cases.

Figure 2 shows the dependence of amplitude $a_0(t)$ calculated according to Eq. (16) versus time at $E = 0$ and at different values of the intersite coupling C. The comparison with the accurate result is also shown ("accurate" result means the numeric integration of Eq. (4).

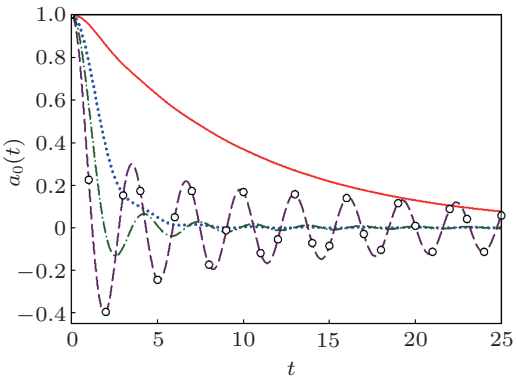


Fig. 2. (color online) The dependence of the amplitude $a_0(t)$, calculated according to Eq. (16), versus time at $E = 0$. Solid line: $C^2 = 0.1$; dotted line: $C^2 = 0.5$; dash-dotted line: $C^2 = 1$; dashed line: $C^2 = 2$. Empty circles: accurate result for $C^2 = 2$, when $a_0(t) = \mathrm{J}_0(2t)$.

The time dependence of the amplitude $a_0(t)$ for small C can be estimated by the Fermi's golden rule, when the perturbation approximation in small parameter C^2 is used, and when an exponential decay occurs,

$$a_0(t) \approx \exp\left(-C^2\sqrt{4-E^2}\,t\right). \quad (18)$$

More accurate expression for the amplitude $a_0(t)$ at small values of parameter C is given in Appendix B.

Now the case when the amplitude $a_0(p)$ has poles is considered. An analysis shows that one pole exists in the domain $E > 2 - C^2$, and two poles, when $E < C^2 - 2$. There are no poles in the domain $|E| < 2 - C^2$ ($C^2 < 2$). Figure 3 shows the number of poles versus the values of parameters E and C.

As an example, we consider the case of one pole in the domain $E > 2 - C^2$ ($C^2 < 2$). The pole is at the point $p = -\mathrm{i}\varepsilon$ ($\varepsilon > 2$). The relation between parameters E and C follows from Eq. (15) as

$$E = \varepsilon\left(1 - \frac{C^2}{2}\right) + \frac{C^2}{2}\sqrt{\varepsilon^2 - 4}. \quad (19)$$

The contribution Δa_0 from the pole is equal to

$$\Delta a_0(t) = \frac{\exp(-\mathrm{i}\varepsilon t)}{1 + \dfrac{C^2}{2}\left(\dfrac{\varepsilon}{\sqrt{\varepsilon^2-4}} - 1\right)}. \quad (20)$$

The full amplitude is then the sum of the leading term (16) and the pole contribution (20). The time dependence of amplitude $|a(t)|$, when one pole exists, is shown in Fig. 4. In this case, the wave function amplitude on the donor does not decrease to zero and $a_0(t)|_{t\to\infty} = 0.75$. It means that 75% of the wave function is captured by the bound state on the donor.

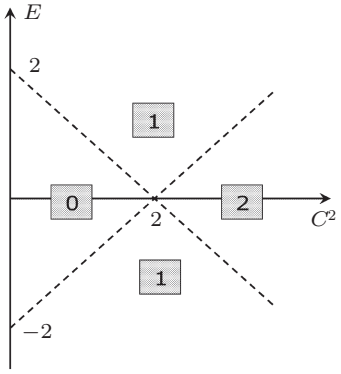


Fig. 3. Number of poles of the integrand of function Eq. (16) in domains divided by dashed lines.

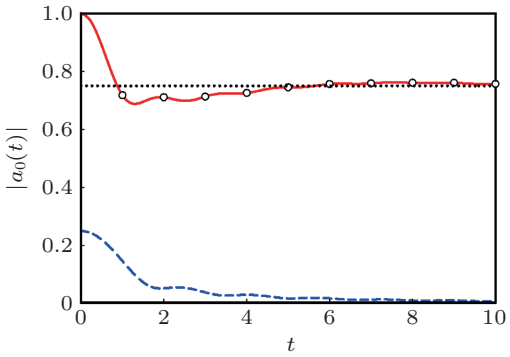


Fig. 4. (color online) The dependence of amplitude $a_0(t)$ on the donor versus time (solid line) in the presence of one pole. Dashed line: contribution to amplitude from the integral summand Eq. (16); dotted line: modulus of the pole summand equal to 0.75 Eq. (20); empty circles: exact numerical result. Parameters: $E = 2$, $C = 1$ ($\varepsilon = 2.5$).

It is shown in Appendix C that if $|E| > 2 - C^2$ ($C^2 < 2$), then there exists the bound state localized at the lattice end on the donor. The value ε (see Eq. (19)) is the energy of this localized state and its contribution to the amplitude $a_0(t)$ coincides with the contribution from the pole summand. Note also that the integral term (16) is the contribution to the amplitude from the continuous spectrum which lies in the interval $[-2, 2]$. A fraction of the initial state is captured by this localized state and the smaller fraction of the initial state goes out to

the reservoir. The effect of returning to the initial state also decreases. This case (existence of a pole) seems less interesting and we consider only an absence of the localized state when the integral (16) is the exact result for amplitude $a_0(t)$.

Such a detailed analysis of the amplitude $a_0(t)$ decaying in the semi-infinite lattice is performed due to two reasons. First, the decay kinetics in the semi-infinite lattice coincides with the kinetic in the finite lattice consisting of N sites in the time range $0 \le t \lesssim N/2$. Second, as will be shown below, the full amplitude in the finite lattice can be represented as a sum of partial amplitudes, the first of which is just the amplitude $a_0(t)$ studied above in such detail.

4. Wave packet spreading through the lattice

In this section, we will consider the quantum dynamics of the wave function on the lattice, i.e., amplitudes $b_j(t)$ variation with time. The moving wave packet gradually gains a well formed shape with a sharp leading front. This behavior is shown in Fig. 5.

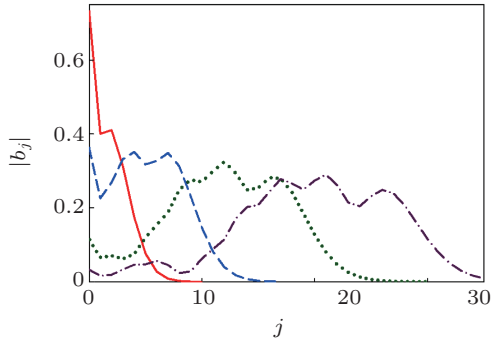


Fig. 5. (color online) Wave packets at different time instants. Here, $t = 2$ (solid line); $t = 5$ (dashed line); $t = 10$ (dotted line); $t = 15$ (dash-dotted line). Site $j = 0$ corresponds to $|a_0(t)|$. Parameters: $E = 1$, $C^2 = 0.5$, $N = 100$. Numerical results coincide with analytical results with very high accuracy and are not shown.

An expression for amplitudes $b_j(t)$ is obtained substituting the expression (8) for the mode amplitudes $b(k,t)$ into expression (6). Then one obtains

$$b_j(t) = -\frac{\mathrm{i}2C}{N+1}\sum_{k=1}^{N}\sin\left(\frac{\pi k}{N+1}\right)\sin\left(\frac{\pi k j}{N+1}\right) \times \exp[-\mathrm{i}\varepsilon(k)t]\int_0^t \exp[-\mathrm{i}\varepsilon(k)\tau]a(\tau)\,\mathrm{d}\tau. \quad (21)$$

Initially, we consider the case of semi-infinite lattice ($N \to \infty$). Changing the summation in Eq. (21) by integration and replacing $a(t)$ by $a_0(t)$, the following expression can be obtained:

$$b_j(t) = -\frac{\mathrm{i}2C}{\pi}\int_0^{\pi}\sin(k)\sin(kj)\exp[-\mathrm{i}\varepsilon(k)t]\,\mathrm{d}k \times \int_0^t \exp[-\mathrm{i}\varepsilon(k)\tau]\,a_0(\tau)\,\mathrm{d}\tau, \quad (22)$$

where $\varepsilon(k) = 2\cos(k)$.

We consider the case when time t is so large that the amplitude $a_0(t)$ becomes very small, $|a_0(t)| \ll 1$. Then the upper limit in the integration over time in Eq. (22) is infinity. The obtained integral is the Laplace transformation $a_0(p)$ taken at $p = -\mathrm{i}\varepsilon(k)$. As a result, we have

$$b_j(t) = -\frac{2C}{\pi}\int_0^{\pi}\frac{\sin(k)\sin(kj)\exp[-2\mathrm{i}t\cos(k)]}{E-2\cos(k)+C^2\exp(-\mathrm{i}k)}\,\mathrm{d}k, \quad |a_0(t)| \ll 1. \quad (23)$$

Expression (23) can be formally generalized on the negative values of index j. Having this in mind, the multiplier $\sin(kj)$ is represented as the difference of two exponentials. Then expression (23) describes the superposition of two wave pulses freely travelling leftward and rightward in the infinite (to both sides) lattice. Every pulse is normalized to unity. We consider separately the wave function pulse running to the right. This pulse is denoted by

$$b_j^{\mathrm{inf}+}(t) = -\frac{\mathrm{i}C}{\pi}\int_0^{\pi}\frac{\sin(k)\exp\{-\mathrm{i}[kj+2\cos(k)t]\}}{E-2\cos(k)+C^2\exp(-\mathrm{i}k)}\,\mathrm{d}k, \quad -\infty < j < +\infty. \quad (24)$$

The considered pulse $b_j(t)$ (in the domain $j > 0$) is the following difference:

$$b_j(t) = b_j^{\mathrm{inf}+}(t) - b_{-j}^{\mathrm{inf}-}(t). \quad (25)$$

The addend $b_{-j}^{\mathrm{inf}-}(t)$ is the "tail" of the pulse $b_j(t)$, and it is small at large times, e.g., $\sim 1/t$. Then $b_j^{\mathrm{inf}+}(t)$ is assumed to be a good approximation for $b_j(t)$. The snapshots of the pulse at different time instants calculated according to Eq. (24) are shown in Fig. 6. One can see that the restriction by the pulse $b_j^{\mathrm{inf}+}(t)$ is a very good approximation.

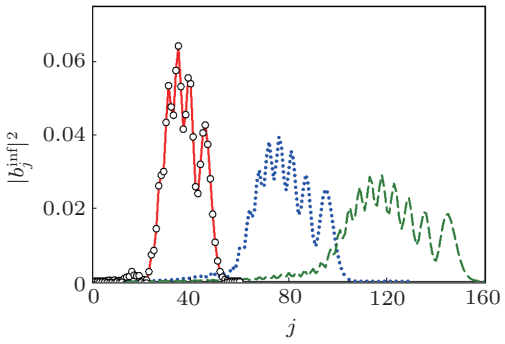


Fig. 6. (color online) Snapshots of the pulse in semi-infinite lattice at $t = 25$ (solid line); $t = 50$ (dotted line); $t = 75$ (dashed line). Calculations according to Eq. (24). Empty circles: numeric integration of Eq. (4). The coincidence of the numeric and analytical results is also very good for $t = 50$ and $t = 75$ (mean square root error (MSRE) $\lesssim 10^{-4}$). Here, $E = 1$, $C = 0.5$, $N = 200$.

Expression $b_j^{\mathrm{inf}+}(t)$ (see Eq. (24)) is a reliable approximation for the spreading pulse on the time interval $t \lesssim N/2$ for the finite but comparatively long lattices. Moreover, as will be demonstrated below, this expression allows one to describe the pulse reflection from the lattice end occurring for the time interval $N/2 \lesssim t \lesssim N$.

We analyze the expression (24) at large time. Because the integrand is the fast oscillating function, the stationary phase method can be applied. If $j < t/2$, then two stationary points exist. They are determined by the equality $\sin(k) = j/2t$, and then the following expression can be obtained:

$$\widetilde{b}_j(t) \approx \frac{-\mathrm{i}C}{\sqrt{\pi t\cos(k_0)}}\Big[f(\pi-k_0) \times \exp(\mathrm{i}\pi/4) + f(\pi-k)\exp(-\mathrm{i}\pi/4)\Big], \quad k_0 \equiv \arcsin(j/2t). \tag{26}$$

Here, $f(k)$ is the integrand in Eq. (24).

Figure 7 shows the comparison of expression (26), obtained in the stationary phase approximation, with the accurate answer.

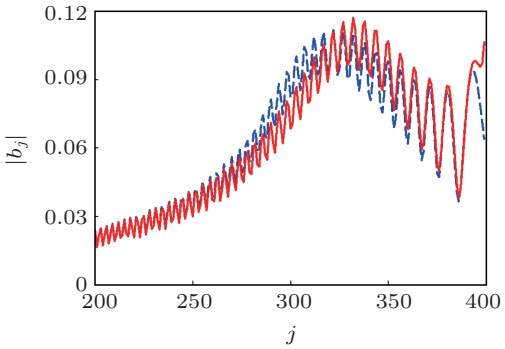


Fig. 7. (color online) The pulse leading edge at $t = 200$. Dashed line represents the numeric result, solid line represents the asymptotic expansion (26). Here, $E = 1$, $C^2 = 2$, $N = 500$.

If $j \approx 2t$, then both stationary points lie close to $k = \pi/2$ and the stationary phase method gives false results (the answer diverges if both points coincide). We consider the region $j \approx 2t$, corresponding to the pulse maximum and its leading edge, in more details. In this case, the expression for amplitudes (24) can be simplified

$$\widetilde{b}_j(t) \approx -\frac{\mathrm{i}C\exp(-0.5\pi j)}{\pi(2-C^2)} \times \int_{-\infty}^{\infty}\frac{\exp\left[\mathrm{i}\left((j-2t)xt^{-1/3}+\frac{1}{3}x^3\right)\right]}{z(t)-x}\,\mathrm{d}x, \quad z(t) \equiv \frac{(E-\mathrm{i}C^2)t^{1/3}}{2-C^2}. \tag{27}$$

If $|z(t)| \gg 1$ (what is valid for $t \gg 1$), then the asymptotic expansion of Eq. (26) can be rewritten as a series in Airy function and its derivatives

$$\widetilde{b}_j(t) \approx -\frac{2\mathrm{i}C}{z(t)(2-C^2)} \times \left[\mathrm{Ai}(\widetilde{j}) + \frac{1}{\mathrm{i}z(t)}\mathrm{Ai}'(\widetilde{j}) - \frac{1}{z^2(t)}\mathrm{Ai}''(\widetilde{j}) + \ldots\right], \quad \widetilde{j} = (j-2t)t^{-1/3}. \tag{28}$$

Thereafter, we can write an approximate expression for the pulse leading edge. Using the asymptotic of the Airy function, one can notice that the dominant term, describing the leading edge, has the form:

$$\widetilde{b}_j(t) \approx -\frac{1}{z(t)}\exp\left\{-\frac{2}{3}\left[(j-2t)t^{-1/3}\right]^{2/3}\right\}. \tag{29}$$

Figure 8 shows the comparison of the asymptotic expansion (28) with the numeric answer.

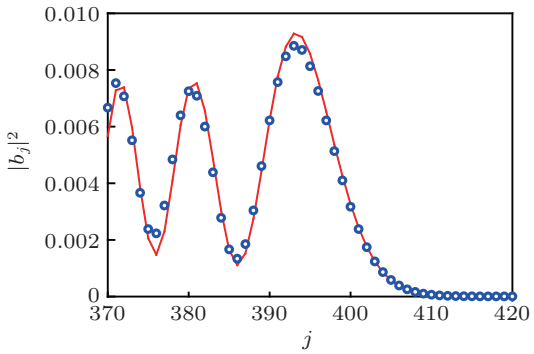


Fig. 8. (color online) The pulse front at $t = 200$ ($E = 1$, $C^2 = 2$). Empty circles: numeric result, solid line: asymptotic expansion (28). Here, MSRE $\lesssim 10^{-3}$.

Expression (29) allows one to describe qualitatively the pulse shape. The dependence on the lattice number j is defined by the argument $(j-2t)t^{-1/3}$. One can notice that the pulse front slowly increases its width $\propto t^{1/3}$ and the amplitude decreases $\propto t^{-1/3}$. This signature becomes apparent only at large values of C and E and at long times. The deviation from this behavior at short times is explained by the fact that the integral in Eq. (27) over x is a number at fixed j and t. The complex value $z(t)$ stands in the denominator with the pole in the complex plane at a distance $\sim C^2 t^{1/3}$ from the real axis. The integral value changes essentially when the asymptotic $|z(t)| \gg 1$ is not fulfilled.

Figure 9 shows the dependence of $\max|b_j(t)|t^{1/3}$ versus time at different C and E values. When $\max|b_j(t)|t^{1/3}$ reaches the constant value, the pulse amplitude becomes $\propto t^{-1/3}$.

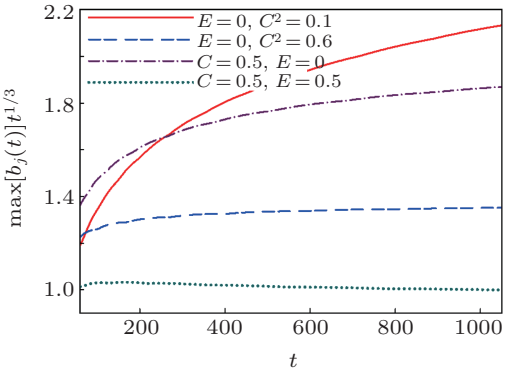


Fig. 9. (color online) Time dependencies of $\max|b_j(t)|t^{1/3}$ at different ("small" and "large") values of E and C shown in insert. The time dependence $\propto t^{-1/3}$ is not fulfilled at $E = 0$, $C^2 = 0.1$, and $C = 0.5$, $E = 0$ even at time $t = 10^3$, but rather quickly ($t \approx 200$) this dependence is satisfied at large E and C. Here, time range $0 \le t \le 1000$, $N = 550$.

The pulse width also changes. The wave packet width can be estimated by the radius of the quantum excitation defined in the considered model as

$$\eta(t) = \frac{1}{|a(t)|^4 + \sum_{j=1}^{N} |b_j(t)|^4}. \tag{30}$$

If the excitation is localized on one site then $\eta = 1$. When the excitation is homogeneously distributed over all sites, i.e. $b_j \sim 1/\sqrt{N}$ then $\eta \sim N$. Figure 10 shows the dependencies $\eta(t)$ at different intersite couplings C. It is easy to notice that the radii of quantum excitations differ significantly for different C values at $t = 500$. The wave packet spreads practically homogeneously over the lattice at $C = 1.25$ and $\eta(t = 500) \approx 325$, while $\eta(t = 500) \approx 38$ at $C = 0.5$. In the latter case the wave packet retains its sharp maximum after travelling an even longer distance (≈ 1000 lattice sites, see insert to Fig. 10).

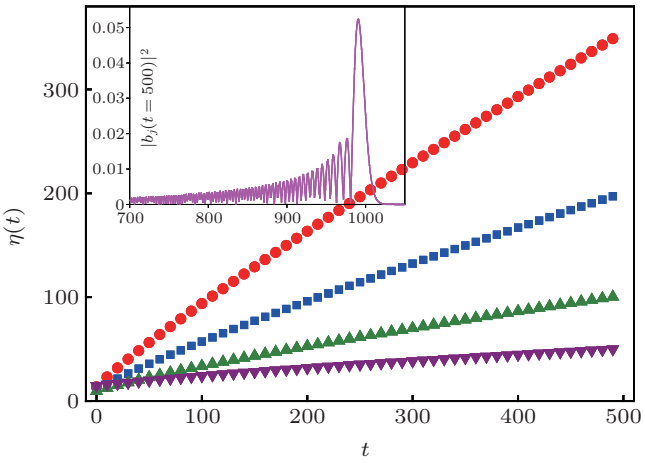


Fig. 10. (color online) Time dependencies of pulse radii $\eta(t)$ at different values of the intercite coupling C. Here, $C = 1.25$ (circles), $C = 1.0$ (squares), $C = 0.75$ (triangles up), $C = 0.5$ (triangles down). Squared modules $|b_j(t)|^2$ at the time instant $t = 2000$ for $C = 0.5$ are shown in the inset. Here, $E = 0$, $N = 550$.

The velocity of the pulse front is 2, maximal possible group velocity. The leading edge has a sharp profile. Thus, if the finite lattice is considered, then until the front achieves the lattice end, its propagation is the same as in the infinite lattice. The pulse front achieves the lattice end at $t \approx N/2$. After that the pulse reflects from the lattice end and the front moves backward to the donor.

Afterwards we consider the pulse reflection. We assume that the lattice is long enough. Then the amplitude $a(t)$ on the donor is negligible and the pulse is fully formed. The pulse leading edge, moving with the velocity $v = 2$, reaches the lattice end at $t \approx N/2$. After reflection it moves with the same velocity $v = 2$ in the opposite direction. At $t \approx N$ the pulse reaches the donor on the left end (see Fig. 1 where the reflected pulse reaches the donor at $t \approx 50$). We consider the pulse evolution at time range $t < N$, when the amplitude $a(t)$ is small and when it coincides with the amplitude $a_0(t)$, the amplitude in the semi-infinite lattice.

5. Pulse reflection

To derive an expression for the reflected pulse we return to the expression (21) for amplitudes $b_j(t)$. We also assume that the time is large enough such that amplitude $a(t)$ is small. Then the upper limit in integration over time is infinity and the substitution $a(t) \to a_0(t)$ is made. As before, the obtained integral can be represented as the Laplace transformation of $a_0(p)$ at $p = -\mathrm{i}\varepsilon(k)$. Then the following expression can be obtained where $b_j(t)$ is represented as a sum

$$b_j(t) = -\frac{2C}{N+1} \sum_{\widetilde{k}=1}^{N} \sin(\widetilde{k}) \sin(\widetilde{k}j) \exp[-2\mathrm{i}t\cos(\widetilde{k})] \times \left[E - 2\cos(\widetilde{k}) + C^2 \exp(-\mathrm{i}\widetilde{k})\right]^{-1}, \tag{31}$$

and $\widetilde{k} = \pi k/(N+1)$.

This expression can be transformed using the Poisson summation formula

$$\sum_{k=-\infty}^{k=\infty} f(k) = \sum_{m=-\infty}^{m=\infty} \int_{-\infty}^{\infty} f(x) \exp(-2\pi\mathrm{i}mx)\,\mathrm{d}x, \tag{32}$$

and the function $f(k)$ differs from zero on the interval $[0, N+1]$. After changing the variables $\pi x/(N+1) \to y$, the following series is obtained:

$$b_j(t) = -\frac{2C}{\pi} \times \sum_{m=-\infty}^{m=\infty} \int_{0}^{\pi} \frac{\sin y \sin(jy) \exp\{-\mathrm{i}[2t\cos y + 2my(N+1)]\}}{E - 2\cos y + C^2\exp(-\mathrm{i}y)}\,\mathrm{d}y. \tag{33}$$

This series can be represented as a sum of two series, expressed through amplitudes b_j^{inf}, amplitudes in the infinite lattice at large time,

$$b_j(t) = \sum_{m=-\infty}^{m=\infty} b^{\mathrm{inf}+}_{j+2m(N+1)}(t) - \sum_{m=-\infty}^{m=\infty} b^{\mathrm{inf}-}_{-j+2m(N+1)}(t). \tag{34}$$

For the separating terms, which are relevant in the considered time domain ($1 \ll t < N$), the expression (24) should be analyzed and those terms, where the phase has the stationary point, should be found. In the first sum the single term with $m = 0$, which describes the incident pulse $b_j^{\mathrm{inf}+}$, is kept. From the second sum, the term with $m = 1$, i.e., $b^{\mathrm{inf}-}_{-j+2(N+1)}$ describing the reflected pulse is kept. Thus, if $t < N$ then the pulse can be represented as the sum of two terms as

$$b_j(t) = b_j^{\mathrm{inf}+}(t) - b^{\mathrm{inf}-}_{-j+2(N+1)}(t). \tag{35}$$

Figure 11 shows the pulse reflection calculated according to Eq. (35). Expression (35) is totally similar to the expression describing the reflection of a wave packet in the continuum case. Indeed, let $\Psi(x,t)$ be a freely propagating wave packet,

and let an infinitely high wall be placed at $x \geq L$ such that the wave function vanishes for $x \geq L$. The needed solution $\Phi(x,t)$ is obvious: $\Phi(x,t) = \Psi(x,t) - \Psi(-x+2L,t)$, which is just the expression (35). In the discrete case, the amplitudes vanish for $j = N+1$.

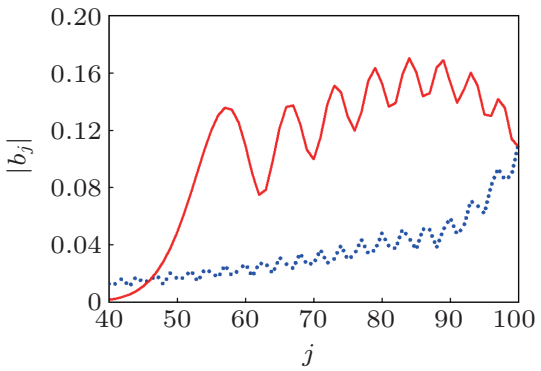


Fig. 11. (color online) Reflection of the pulse from the lattice end. $t = 75$. Computation according to Eq. (35). Solid line is the reflected pulse, dotted line represents the tail of the incident pulse. At $t = 75$ the pulse leading edge, moving with $v = 2$, passed ≈ 150, lattice sites: 100 sites before reflection and 50 sites after reflection, MSRE $< 10^{-4}$ (numeric data are not shown), $E = 1$, $C^2 = 0.5$, $N = 100$.

At the instant $t \approx N$ the pulse leading edge returns to the lattice beginning and starts to interact with the donor. Amplitude $a(t)$ increases. Our approximation concerning the smallness of $a(t)$ becomes invalid. The system begins its return to the initial state. This process is analyzed in the next section.

6. Wave packet recurrence

Starting from the initial condition $a(t=0) = 1$ the pulse, having the well formed shape, spreads through the lattice with the velocity $v = 2$. If the lattice consists of N sites, then the time of the first returning to the donor is $t \approx N$. The cycle of k recurrences takes time $t \approx kN$. We solve the Eq. (9) with the kernel given by Eq. (10) to find $a(t)$ at any time within arbitrary recurrence cycle k. The solution is searched in the form of the expansion in terms of partial amplitudes $a_k(t)$. The condition is imposed that each of amplitudes $a_k(t)$ is negligible in the time range $t \lesssim kN$ and its contribution to the total amplitude $a(t)$ becomes essential only starting from times $t \sim kN$, i.e., after the k-th recurrence.

In order to make sure in this kind of possibility, the kernel $B^N(t)$ (Eq. (10)) is transformed according to the Poisson summation formula

$$B^N(t) = C^2 \sum_{m=-\infty}^{\infty} B_m(t),$$

where

$$B_m(t) = \frac{2}{\pi} \int_0^{\pi} \sin^2(x) \exp\{-2\mathrm{i}\,[m(N+1) + t\cos(x)]\}\,\mathrm{d}x. \tag{36}$$

We emphasize that $B_m(t)$ is the real function and recall that there exists the explicit expression for $m = 0$ through Bessel functions

$$B_0(t) = \mathrm{J}_0(2t) + \mathrm{J}_2(2t). \tag{37}$$

Afterwards the original Eq. (9) with regard to transformation (36) takes the form

$$\dot{a}(t) = -\mathrm{i}Ea(t) - C^2 \sum_{m=-\infty}^{\infty} \int_0^t B_m(t-\tau)\,a(\tau)\,\mathrm{d}\tau. \tag{38}$$

Note an important and useful property of functions B_m: every function $B_m(t)$ is small in the time range $0 < t < mN$, such that

$$B_m(t) \approx \frac{\sin(2t)}{\pi[m(N+1)]^3}, \quad m(N+1) - t \gg 1. \tag{39}$$

With a reasonable degree of accuracy one can say that the function $B_m(t) \approx 0$ when $t < mN$. Consequently, when $t < mN$, then only terms B_k with indices $k < m$ give an essential contributions to Eq. (38).

Now we represent amplitude $a(t)$ as the sum of partial amplitudes

$$a(t) = a_0(t) + a_1(t) + a_2(t) + \cdots. \tag{40}$$

Recall that the assumption concerning amplitudes $a_k(t)$ is based on the fact that amplitudes $a_k(t)$ are small at $t < kN$. To some extent $a_k(t)$ behaves like $B_k(t)$. Deriving an equation for $a_k(t)$ we assume that its right-hand side contains only terms $B_m(t)$ with $m \leq k$.

Prior to writing down an equation for $a_k(t)$, we make one comment. Terms $B_m(t)$ are small (even for not too long lattices). This smallness is ensured by the fact that $B_{-m}(t) = B_m(-t)$, and $B_m(t) \sim (mN)^{-3}$ in the considered time range ($t > 0$). Nevertheless terms with negative indices m are taken into account as their accounting allows one to derive explicit analytical formulaes.

We introduce functions $\widetilde{B}_m(t)$ to account for the contributions from $B_m(t)$ ($m < 0$)

$$\widetilde{B}_m(t) = B_m(t) + B_{-m}(t), \quad m > 0, \tag{41}$$

and we set $\widetilde{B}_0(t) \equiv B_0(t)$ for the uniformity of notations.

Now in accordance with our assumptions, we convert Eq. (38) in a system of cycling equations for partial amplitudes $a_k(t)$. The equation for $a_0(t)$ contains only function $\widetilde{B}_0(t)$ in the right-hand side (see Eq. (37))

$$\dot{a}_0(t) = -\mathrm{i}Ea_0(t) - C^2 \int_0^t \widetilde{B}_0(t-\tau)\,a_0(\tau)\,\mathrm{d}\tau, \quad a_0(0) = 1, \tag{42}$$

and taking into account the above-mentioned arguments, an equation for $a_k(t)$ ($k > 0$) can be rewritten

$$\dot{a}_k(t) = -\mathrm{i}Ea_k(t) - C^2 \int_0^t \sum_{m=0}^{k} \widetilde{B}_m(t-\tau)\,a_{k-m}(\tau)\,\mathrm{d}\tau,$$

$$a_k(0) = 0\ (k>0). \tag{43}$$

It is important to note that system (43) is exact.

The Laplace transformation of Eq. (42) gives the following expression for $a_0(p)$:

$$a_0(p) = \frac{1}{p+\mathrm{i}E+C^2\widetilde{B}_0(p)}. \tag{44}$$

Here, $\widetilde{B}_0(p)$ is the Laplace transform of $B_0(t)$

$$\widetilde{B}_0(p) = \frac{1}{2}\left(\sqrt{p^2+4}-p\right). \tag{45}$$

Expression (44) is nothing else but the amplitude $a(t)$ in the semi-infinite lattice when there are no reflections (see Section 3).

The Laplace transformation of system (43) gives the algebraic system of recurrence relationships for $a_k(p)$ $(k>0)$

$$a_k(p) = -C^2 a_0(p)\sum_{m=0}^{k-1}\widetilde{B}_{k-m}(p)\,a_m(p). \tag{46}$$

The Laplace transform $\widetilde{B}_m(p)$ of the function $\widetilde{B}_m(t)$ is given by the integral

$$\widetilde{B}_m(p) = \frac{2}{\pi}\int_0^t \sin^2 y \exp[-2\mathrm{i}m(N+1)y] \times\left[\frac{1}{p+2\mathrm{i}\cos y}+\frac{1}{p-2\mathrm{i}\cos y}\right]\mathrm{d}y. \tag{47}$$

An explicit form of this integral can be obtained. With this aim in view, the integration contour is deformed as shown in Fig. 12. As the integrand in Eq. (47) has period π, integrals I_1 and I_2 are cancelled as they have opposite integration paths. Consequently $\widetilde{B}_m(p)$ is defined only by the pole contribution at the point y_0 $(\cos(y_0) = \mathrm{i}p/2)$. Then we have

$$\widetilde{B}_m(p) = \sqrt{4+p^2}\left[\mathrm{i}\widetilde{B}_0(p)\right]^{2m(N+1)}. \tag{48}$$

Due to the fact that $\widetilde{B}_m(p)$ forms the geometrical progression by m, it is possible to make an explicit summation in recurrence formulaes (46). This is the main reason why the total amplitude $a(t)$ can be represented in the form of the closed expression (see Appendix D).

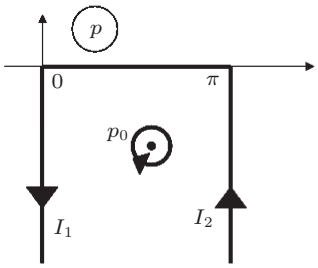


Fig. 12. The integration along the path $[0,\pi]$ in expression (47) is changed to the residue in the pole p_0 and two integrals I_1 and I_2.

The Laplace transforms of the partial amplitudes $a_k(p)$ $(k>0)$ are expressed as

$$a_k(p) = -a_0(p)\,d\,(1-d)^{k-1}\left(\mathrm{i}\widetilde{B}_0\right)^{2k(N+1)}, \quad \text{where}\quad d \equiv a_0(p)C^2\sqrt{p^2+4}. \tag{49}$$

To get explicit expressions for the partial amplitudes, the inverse Laplace transform is made. Transforming the Laplace integral to the integration path around the cut $[-2\mathrm{i}, 2\mathrm{i}]$, one gets an expression for $a_0(t)$

$$a_0(t) = \frac{1}{\pi}\int_{-2}^{2}\exp(\mathrm{i}xt)\,\mathrm{Im}\left\{\left[x\left(1-\frac{C^2}{2}\right)+E-\mathrm{i}\frac{C^2}{2}\sqrt{4-x^2}\right]^{-1}\right\}\mathrm{d}x. \tag{50}$$

Further on, we get expressions for partial amplitudes $a_k(t)$ as

$$a_k(t) = -\frac{C^2}{\pi}\int_{-2}^{2}\sqrt{4-x^2}\exp(\mathrm{i}xt) \times \mathrm{Re}\left[a_0^2\left(1-C^2a_0\sqrt{4-x^2}\right)^{k-1}\left(\mathrm{i}\widetilde{B}_0\right)^{2k(N+1)}\right]\mathrm{d}x. \tag{51}$$

Here, the Laplace transform for $a_0(p)$ is performed at $p=\mathrm{i}x$. An analysis of the expression for $a_k(t)$ shows that, as supposed, $a_k(t) \ll 1$ when $t < (k+1)N$.

Therefore, if the partial sum $a_0 + a_1 + \cdots + a_k$ is taken for the representation of amplitude $a(t)$, then the error of such approximation is of the same order as the smallness of $\widetilde{B}_k(t)$, i.e., $\sim[(k+1)(N+1)]^{-3}$.

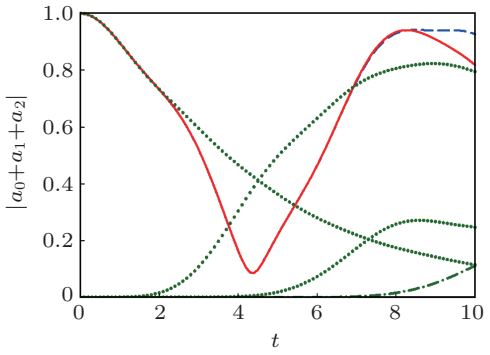


Fig. 13. (color online) The comparison of partial amplitudes sum $|a_0|+|a_1|+|a_2|$ (solid line) with the numeric integration (dashed line). Dotted lines: partial amplitudes $|a_0|$, $|a_1|$, $|a_2|$ "starting" at times $t=0,2,4$, correspondingly. A small divergence is observed only at $t>8$ where the unaccounted partial amplitude $|a_4|$ (dash-dotted line) starts to contribute. Parameters: $N=2, E=1, C=0.5$, MSRE $\lesssim 10^{-4}$.

Consider as an example, the most unfavorable case of a very short lattice $(N=2)$, and as an approximation, the sum of only three partial amplitudes $a_0+a_1+a_2$. In Fig. 13 this partial sum is compared with the exact result of the numeric

integration of the system (4). For $t < 8$ the expected error is $\sim 5 \times 10^{-5}$. Thus the representation of $a(t)$ by the sum of partial amplitudes is a very good approximation even for short lattices (the accuracy increases if the lattice becomes longer).

7. Multiple returning to the initial state

If the lattice is long enough then partial amplitudes, following each other, have enough time for damping on the corresponding time ranges $[t, t+N]$. In this case partial amplitudes do not interfere and reproduce the total amplitude with very high accuracy (see Fig. 1). The maxima of returning amplitudes slowly decrease.

Partial amplitudes interfere on short lattices and maxima of returning amplitudes are irregular. The dependence of the total amplitude $a(t)$ versus time for the lattice with $N = 10$ is shown in Fig. 14. Numeric analysis performed at different values of parameters C, E, and N shows, that the maximal value of returned amplitude is $a_{\max} \approx 0.972$ at $t = 42$ for $N = 10$.

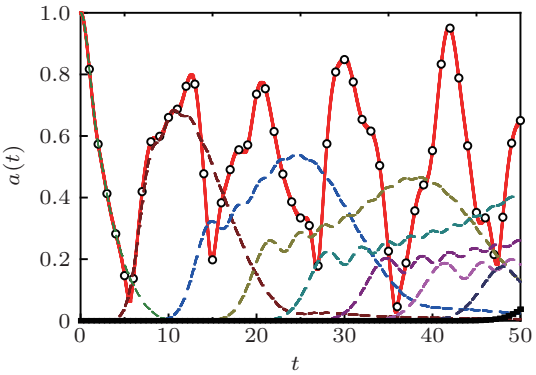


Fig. 14. (color online) Solid line: sum of partial amplitudes $|a_0(t)| + |a_1(t)| + \cdots + |a_8(t)|$. Dashed lines: partial amplitudes $|a_0|, |a_1|, \ldots, |a_8|$ starting approximately at time instants $t_k = (N/2)k = 5k$, $k = 0, 1, \ldots, 8$. Maximal value of returned amplitude is ≈ 0.97 at $t = 42$. Empty circles: numeric results, MSRE $\lesssim 10^{-5}$. Parameters: $N = 10$, $E = 0$, $C^2 = 0.4$.

Incident and reflected pulses interfere on short lattices and the degree of returning is difficult to analyze at arbitrary parameter values C, E, N, but the first returning (maximal value of the partial amplitude $a_1(t)$) can be treated analytically if the lattice is long enough when the amplitude $a_0(t)$ becomes negligible.

The expression (51) for $a_1(t)$ using the trigonometric substitution of variables can be rewritten as

$$a_1(t) = \frac{4C^2}{\pi} \int_0^{\pi} \sin^2(x) \exp[2\mathrm{i}t\cos(x)] \times \mathrm{Re}\left\{ \frac{\exp[2\mathrm{i}(N+1)x]}{[2\cos(x) + E - C^2\exp(\mathrm{i}x)]^2} \right\} \mathrm{d}x. \quad (52)$$

Figure 15 shows the maximal values of amplitude $|a_1(t)|$ calculated according to Eq. (52) at $E = 0$ and different values of parameters N and C. One can notice that if $C^2 \approx 0.2$ then the returned amplitude practically does not depend on the lattice length ($10 < N < 100$). The dissimilarity of the partial amplitude $a_1(t)$ from the total amplitude $a(t)$ is negligible on this time range ($N < t < 2N$). The divergence becomes essential ($\sim 15\%$) for the shortest of considered lattices ($N = 10$) and the smallest value of parameter C ($C^2 = 0.1$). Amplitude $a_0(t)$ has not enough time to fully decay at these parameters values, and interferences with $a_1(t)$.

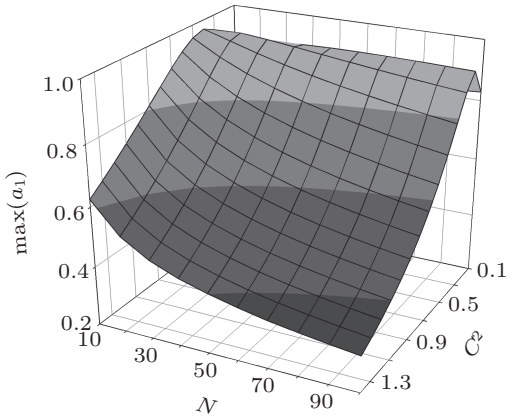


Fig. 15. Maximal value of amplitude of the first returning $a_1(t)$ at $E = 0$ and different values of C and N.

8. Conclusions

The wave function pulse, responsible for the charge propagation through the lattice, moves starting from the donor at the lattice end. If the electronic excitation is totally localized on the donor then, depending on the donor parameters, few scenarios of the quantum dynamics are realized. One of the most common cases is the formation of a pulse and its spreading through the lattice. The pulse moves with the maximal group velocity $v = 2$ and has the steep leading edge. The pulse amplitude decreases $\propto t^{-1/3}$ and the width increases $\propto t^{1/3}$. After reaching the opposite lattice end, the pulse reflects and moves in the opposite direction. This process can repeat many times.

The other scenario is realized if the parameters of the donor are such that the bound state is formed. Then the wave function is partially captured by this bound state. The analytical expressions describing the impulse dynamics coincide with the accurate numeric simulation with high precision.

There are several functions which describe the charge transfer employing the wave packet amplitudes $b_j(t)$. These include the first: $M_1(t) = \sum_{j=1}^{N} j\,|b_j(t)|^2$ and second: $M_2(t) = \sum_{j=1}^{N} j^2\,|b_j(t)|^2$ moments, and mean squared displacement $\sigma(t) = \sqrt{\sum_j [j - \langle n(t)\rangle]^2\,|b_j(t)|^2}$, where $\langle n(t)\rangle = \sum_j j\,|b_j(t)|^2$.[20]

Different dependencies for probabilities and velocities of the pulse spreading are obtained as functions of the models used, and their parameters. Usually the dependence $M_2(t) \propto t^{\beta}$ is fulfilled. The power index β falls within the range $0 < \beta \leq 2$. The ballistic transport ($\beta = 2$) is realized in the considered case of the defect-free lattice. If the lattice has the diagonal or/and off-diagonal disorder, then $\beta < 2$ and one or the other diffusion behavior is observed. Unusual hyperdiffusion cases when $\beta > 2$ are also known.[41,42] The second moment $M_2(t)$ is mostly calculated numerically, integrating the system similar to Eq. (4). Functions $M_2(t)$ and $\sigma(t)$ can be calculated explicitly as there exist analytical representations for wave function amplitudes $b_j(t)$ in the present paper.

The problem of the electronic excitation spreading through the lattice formulated in a rather simple form, can be relevant to recent experiments on the charge transfer in synthetic olygonucleotides, polypeptides, and other non-metallic systems. At one time, it seemed that the polaron mechanism can adequately explain the charge transport in such substances.[43–50]

However, at least two weak points in the polaronic paradigm exist. First, polaron formation. After a charge is transferred to the chain, it should be more or less localized for some time allowing the polaron formation. The characteristic "dynamical" time of the lattice rearrangement ($\sim \sqrt{m/k}$) is approximately two orders of magnitude greater compared to the "quantum" time ($\sim \hbar/\xi$); k, m are lattice rigidity and the mass of a particle, and ξ, intersite coupling. Otherwise, as is observed in numerical simulations, the wave function spreads very fast and approximately homogeneously along the lattice. The reason is that the lattice has not enough time for self-arranging and the polaron has no time for self-trapping. Most of the previous studies considered the polaron evolution on lattices with different interaction potentials when a polaron was created "by hand" as an initial condition. Unfortunately, too little attention was paid to the mechanisms of polaron formation.

The second problem is how the polaron can get an initial momentum necessary for the coherent movement. The initially formed unmovable polaron can start to move randomly (one-dimensional random walk) only under the influence of thermal fluctuations. Its diffusive movement cannot explain the experimentally observed single-step coherent transport.[9] As to our best knowledge, there exists the unique mechanism obeying the movement: When the next-to-nearest-neighbour interactions are included, for physical values of the parameters, polarons can spontaneously move, at $T = 0$, on bent chains that exhibit a positive gradient in their curvature.[51]

The discussed mechanism of quantum dynamical charge transfer allows one to exclude these difficulties in explaining the highly efficient charge transfer over long distances: the electronic wave packet, responsible for the charge transport, spontaneously forms and moves.

It is worth noting that results derived above for the defect-free lattices are also valid for weakly disordered systems. It was numerically verified that the pulse, travelling through the lattice $N = 200$ with the diagonal disorder $W = 1$, preserves its shape with rather good accuracy and is well approximated by Eq. (27).

Appendix A

The expression for amplitude $a_0(t)$ (see Eq. (15)) can be rewritten in the following form:

$$a_0(t) = \frac{C^2}{2\pi} \int_{-2}^{2} \frac{\sqrt{4-\omega^2}\exp(\mathrm{i}\omega t)}{(\omega+E)(\omega+E-\omega C^2)+C^4}\,\mathrm{d}\omega. \tag{A1}$$

This expression can be transformed to the differential equation by time. It can be done if the denominator of the integrand can be represented as the differential operator with the replacement $\omega \to -\mathrm{i}\mathrm{d}/\mathrm{d}t$. Then the action of this differential operator on both sides of Eq. (A1) eliminates the denominator. The resulting integral is expressed through the Bessel functions. As a result, the following differential equation is obtained:

$$\begin{aligned}&(1-C^2)\ddot{a}_0(t) + \mathrm{i}E(2-C^2)\dot{a}_0(t) - (C^4+E^2)a_0(t)\\ &= -C^2\left[\mathrm{J}_0(2t)+\mathrm{J}_2(2t)\right].\end{aligned} \tag{A2}$$

It is the inhomogeneous linear differential equation of the second order. Initial conditions for this equation are: $a_0(t=0) = 1$ and $\mathrm{d}a_0/\mathrm{d}t|_{t=0} = -\mathrm{i}E$ (this condition follows from Eq. (12)).

The solution of this equation can be formally written as the integral over time, but this integral is difficult to evaluate analytically and numeric calculation is more complex compared to the original expression (13). Nevertheless, it can be shown that the solution can be represented through Bessel functions, and few particular cases exist when the solution can be written in a rather compact form.

If $C = 1$, then equation (A2) is the first-order equation. Its solution can be expanded into a series in Bessel functions

$$\begin{aligned}a_0(t) &= \mathrm{J}_0(2t) - \mathrm{i}E\mathrm{J}_1(2t) + (1-E^{-2})\\ &\times \sum_{k=2}^{\infty}(-\mathrm{i}E)^k \mathrm{J}_k(2t).\end{aligned} \tag{A3}$$

In the case of $E = 0$, equation (A2) has no first-order derivative and its solution is a series in even Bessel functions

$$a_0(t) = \mathrm{J}_0(2t) + (2-C^2)\sum_{k=1}^{\infty}(1-C^2)^{k-1}\mathrm{J}_{2k}(2t). \tag{A4}$$

In the general case, the solution of Eq. (A2) can be written as the series

$$a_0(t) = \mathrm{J}_0(2t) - \mathrm{i}E\mathrm{J}_1(2t) - \frac{C^2}{2p(1-C^2)}$$

$$\times \sum_{k=2}^{\infty} \left[q_1 (r_1)^k - q_2 (r_2)^k \right] \mathrm{J}_k(2t), \qquad \text{(A5)}$$

where

$$p = \sqrt{\frac{E^2 + C^4}{1 - C^2} - \left[\frac{2 - C^2}{2(1 - C^2)} \right]^2},$$
$$p_1 = p - \mathrm{i} \frac{2 - C^2}{2(1 - C^2)}, \quad p_2 = -p_1^*,$$
$$q_i = \frac{4 + p_i^2}{p_i^2 + 2 - p_i r_i}, \quad i = 1, 2,$$
$$r_i = \frac{1}{2} \left(p_i \pm \sqrt{4 + p_i^2} \right), \quad i = 1, 2. \qquad \text{(A6)}$$

Sign for r_i in Eq. (A6) is chosen such that $|r_i| < 1$.

Appendix B

When the intersite coupling C is small then the amplitude $a_0(t)$ on the donor slowly exponentially decays. Below we get two approximate expressions for the amplitude $a_0(t)$ when $C \ll 1$.

The first method consists in modifying the integral formula Eq. (16) for $a_0(t)$. This expression can be rewritten as

$$a_0(t) = \frac{C^2}{2\pi} \int_{-2}^{2} \frac{\sqrt{4 - \omega^2} \exp(\mathrm{i}\,\omega t)}{(\omega + E)(\omega + E - \omega C^2) + C^4} \mathrm{d}\omega. \qquad \text{(B1)}$$

If C is small then an approximate expression for $a_0(t)$ can be derived from Eq. (B1). To do this, the integration contour in Eq. (B1) should be deformed as shown in Fig. B1. In the upper semiplane, the integrand in Eq. (B1) has a pole at the point $\omega = \omega_1$,

$$\omega_1 = \frac{1}{2(1 - C^2)} \left[-E(2 - C^2) + \mathrm{i} C^2 \sqrt{4 - 4C^2 - E^2} \right]. \qquad \text{(B2)}$$

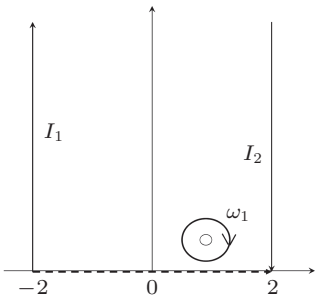


Fig. B1. The transformation of the initial integral Eq. (B1) (dashed line $[-2, +2]$) into two integrals $I_1 \in [-2; -2 + \mathrm{i}\infty]$, $I_2 \in [2; 2 + \mathrm{i}\infty]$ and the residue in the pole $\omega = \omega_1$.

When $C \ll 1$, then the pole lies very close to the real axis (on the distance $\sim C^2$). Therefore, the contribution of the pole term decreases with time very slowly, slower than the contribution from integrals I_1 and I_2.

The reason is that integrals I_1 and I_2 contain the exponentially decaying multiplier $\exp(-\omega t)$. Therefore, at large time the contribution from these integrals is small in comparison with the contribution from the pole. Thus, at small C and taking into account only the pole contribution, we obtain the following approximate expression for the amplitude decay:

$$a_0(t) \approx \exp(\mathrm{i}\,\omega t) \sqrt{\frac{4 - \omega_1^2}{4 - 4C^2 - E^2}}. \qquad \text{(B3)}$$

At small C, the expression for the amplitude can be additionally simplified and the result coincides with Fermi's golden rule

$$a_0(t) \approx \exp\left[\left(-\mathrm{i}E - \frac{1}{2} C^2 \sqrt{4 - E^2} \right) t \right]. \qquad \text{(B4)}$$

Another approximate expression for the amplitude $a_0(t)$ (at $C \ll 1$) can be derived using the perturbation theory for the initial equation (Eq. (12))

$$\dot{a}_0(t) = -\mathrm{i}E a_0(t) - C^2 \int_0^t B_0(t - \tau) a_0(\tau) \mathrm{d}\tau,$$
$$B_0(t) = \mathrm{J}_0(2t) + \mathrm{J}_2(2t). \qquad \text{(B5)}$$

We introduce the function $\widetilde{a}_0 = a_0 \exp(\mathrm{i}Et)$. For this function, we have the following equation:

$$\frac{\mathrm{d}\widetilde{a}_0}{\mathrm{d}t} = -C^2 \int_0^t B_0(t - \tau) a_0(\tau) \mathrm{d}\tau. \qquad \text{(B6)}$$

The function $\widetilde{a}_0(t)$ varies slowly at small C, and in the first-order of the perturbation theory we can put $\widetilde{a}_0(\tau) \approx a_0(\tau)$ in the integrand. As a result the linear differential equation can be obtained. Its solution is

$$\widetilde{a}_0(t) = \exp\left[-C^2 \int_0^t (t - \tau) \exp(\mathrm{i}E\tau) [\mathrm{J}_0(2\tau) + \mathrm{J}_2(2\tau)] \mathrm{d}\tau \right]. \qquad \text{(B7)}$$

Note that this expression is valid when time t is small. If $t \gg 1$ then expression (B7) can be additionally simplified. Evaluating the corresponding integrals and returning back to the function $a_0(t)$, we obtain

$$a_0(t) = \exp\left[\frac{C^2}{2} - \frac{C^2 \sqrt{4 - E^2}}{2} t - \mathrm{i}E \left(1 + \frac{C^2}{2} \right) t + \frac{\mathrm{i}EC^2}{2\sqrt{4 - E^2}} \right]. \qquad \text{(B8)}$$

Note that the error estimation of the exponent shows that this error is of the order not exceeding $t^{-3/2}$.

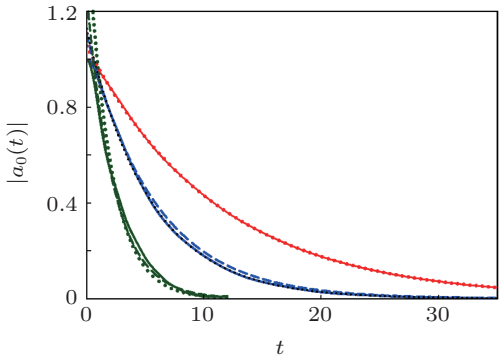


Fig. B2. (color online) The dependence of the amplitude $|a_0(t)|$ decay versus time, $E = 1$. Parameter C from up to down in the figure: $C^2 = 0.1$; 0.2; 0.5. Solid lines: numeric results; dashed lines: the pole approximations Eq. (B3); dotted lines: the perturbation theory Eq. (B8).

It should also be pointed out that expression (B8) for $a_0(t)$ gives an answer coinciding with Fermi's golden rule (but with the extra multiplier $\exp(C^2/2)$ in expression (B8)). Figure B2 shows the comparison of the numeric answer for the amplitude $a_0(t)$ decays with the approximate expressions (B3) and (B8).

Appendix C

Consider now the case when $E > 2 - C^2$ ($C^2 < 2$) and when there exists one localized bound state. We find the eigenfunction $\boldsymbol{\Psi}_{\rm loc}$ localized at the lattice end (electron donor) and solve the Schrödinger equation $\boldsymbol{H}\boldsymbol{\Psi}_{\rm loc} = \varepsilon\boldsymbol{\Psi}_{\rm loc}$ (for the Hamiltonian $\boldsymbol{H}$ see Eq. (2)). The solution has the form of the exponentially decaying function of j

$$\boldsymbol{\Psi}_{\rm loc} = A\left\{\frac{1}{C}, \alpha^{j-1}\right\}, \quad A = \left(\frac{1}{C^2} + \frac{\alpha^2}{1-\alpha^2}\right)^{-1/2}. \tag{C1}$$

Parameter α is expressed through the energy ε

$$\alpha = \frac{1}{2}\left(\varepsilon - \sqrt{\varepsilon^2 - 4}\right). \tag{C2}$$

Energy ε is related to parameters E and C by the relationship, coinciding with Eq. (17)

$$E = \varepsilon\left(1 - \frac{C^2}{2}\right) + \frac{C^2}{2}\sqrt{\varepsilon^2 - 4}. \tag{C3}$$

Expand now the total wave function in terms of the eigenfunctions of the Hamiltonian

$$\boldsymbol{\Psi} = D\boldsymbol{\Psi}_{\rm loc}\exp(-{\rm i}\varepsilon t) + {\rm CCS}, \tag{C4}$$

where CCS means the contribution from the continuous spectrum. The first term is just the contribution to amplitude from the localized state. It is necessary to find the constant D. To do this we consider the scalar product of the localized and the total wave functions. Because of the orthogonality of wave functions one gets $\langle\boldsymbol{\Psi}_{\rm loc}\boldsymbol{\Psi}\rangle = D\exp(-{\rm i}\varepsilon t)$. In this equality we put $t = 0$. As the wave function is localized on the donor at $t = 0$, i.e., $\boldsymbol{\Psi}(t=0) = (1,0,0,\ldots)$, then $D = \boldsymbol{\Psi}^*_{\rm loc}(j=1)$. Thus, the necessary contribution to the amplitude on the donor from the localized state is

$$a_0^{\rm loc} = |\boldsymbol{\Psi}_{\rm loc}(1)|^2\exp(-{\rm i}\varepsilon t). \tag{C5}$$

Substituting the expression $\boldsymbol{\Psi}_{\rm loc}(1) = AC^{-1}$ from Eq. (C1) and expressing A through ε (see Eq. (C2)) we obtain the final answer, coinciding with Eq. (17),

$$a_0^{\rm loc}(t) = \frac{\exp(-{\rm i}\varepsilon t)}{1 + \dfrac{C^2}{2}\left(\dfrac{\varepsilon}{\sqrt{\varepsilon^2-4}} - 1\right)}. \tag{C6}$$

Appendix D

The original equation for the amplitude $a(t)$ has the form (see Eq. (9))

$$\dot{a}(t) = -{\rm i}Ea(t) - C^2\int_0^t B^N(t-\tau)a(\tau)\,{\rm d}\tau,$$
$$a(t=0) = 1. \tag{D1}$$

The solution of this equation for the Laplace transform $a(p)$ is

$$a(p) = \frac{1}{p + {\rm i}E + B^N(p)}. \tag{D2}$$

The Poisson representation for the kernel $B^N(p)$ has the form

$$B^N(p) = C^2\sum_{m=0}^{\infty}\widetilde{B}_m(p),$$
$$\widetilde{B}_0(p) = \frac{1}{2}\left(\sqrt{p^2+4} - p\right),$$
$$\widetilde{B}_m(p) = \sqrt{p^2+4}\,[b(p)]^{2m(N+1)}, \quad m > 0, \tag{D3}$$

where the notation

$$b(p) \equiv \left({\rm i}\widetilde{B}_0(p)\right)^{2k(N+1)} \tag{D4}$$

is introduced. On account that values $\widetilde{B}_m$ form the geometrical progression, one obtains

$$B^N(p) = C^2B_0(p) + C^2\sqrt{p^2+4}\frac{b(p)}{1-b(p)}, \tag{D5}$$

and the final expression for the total amplitude is

$$a(p) = a_0\frac{1-b(p)}{1 + b(p)\left(C^2a_0(p)\sqrt{p^2+4} - 1\right)}. \tag{D6}$$

An expansion into series in terms by $b(p)$ gives Laplace transforms of partial amplitudes. By these means, it was not necessary to construct the system of the recurrence relations for the partial amplitudes, but simply use the expansion $a(p)$ Eq. (D6) into a series in terms by $b(p)$. However, this approach is valid only for the considered model where the necessary summation is possible and the compact expression for the kernel B^N can be written. The method suggested in the paper of the expansion into a series by partial amplitudes can be applied in general cases.

The back Laplace transformation gives a necessary expression for $a(t)$

$$a(t) = \frac{1}{2\pi} \int_{-\infty}^{\infty} a(p)\,\mathrm{d}p, \quad p = \Delta + \mathrm{i}\,\omega, \quad \Delta > 0. \tag{D7}$$

Numerically, it was verified that expression (D7) gives accurate results.

It worth noting one intriguing property. If the integration path expression (D7) is closed around the cut $[-2\mathrm{i}, 2\mathrm{i}]$, then the result (difference of integrals taken along banks of the cut) is zero. It was found numerically. It follows that the function $a(p)$ has poles in the complex plane. Amplitude $a(t)$ can be obtained as the sum of residues in these poles. Additional analysis is necessary to throw light on this fact.

References

[1] Eberhard S, Finazzi G and Wollmann F A 2008 *Annu. Rev. Genet.* **42** 463
[2] Burda K 2007 *Cell Biochem. Biophys.* **47** 271
[3] Ferreira K N, Iverson T M, Maghlaoui K, Barber J and Iwata S 2004 *Science* **303** 1831
[4] Loll B, Kern J, Saenger W, Zouni A and Biesiadka J 2005 *Nature* **438** 1040
[5] Rich P R 2003 *Biochem. Soc. Trans.* **31** 1095
[6] Verkhovskaya M L, Belevich N, Euro L, Wikström M and Verkhofsky M 2008 *Proc. Natl. Acad. Sci. USA* **105** 3763
[7] Augustyn K E, Genereux J C and Barton J K 2007 *Angew. Chem. Int. Ed.* **46** 5731
[8] Barton J K, Olmon E D and Sontz P A 2011 *Coord. Chem. Rev.* **255** 619
[9] Genereux J C and Barton J K 2010 *Chem. Rev.* **110** 1642
[10] Mallajosyula S S and Pati S K 2010 *J. Phys. Chem. Lett.* **1** 1881
[11] Giese B 2002 *Annu. Rev. Biochem.* **71** 51
[12] Slater C and Koster G F 1954 *Phys. Rev.* **94** 1498
[13] Anderson P W 1958 *Phys. Rev.* **109** 1492
[14] Biswas P, Cain P, Römer R A and Schreiber M 2000 arXiv:cond-mat/0001315[cond-mat.dis-nn]
[15] Kantelhardt J W, Berkovits R, Havlin S and Bunde A 1999 *Physica A* **266** 461
[16] Kohmoto M, Sutherland B and Tang C 1987 *Phys. Rev. B* **35** 1020
[17] Ludlam J J, Taraskin S N and Elliott S R 2003 *Phys. Rev. B* **67** 122203
[18] Milde F, Römer R A and Schreiber M 1997 *Phys. Rev. B* **55** 9463
[19] Flach S 2010 *Chem. Phys.* **375** 548
[20] de Moura F A B F, Caetano R A and Santos B 2012 *J. Phys.: Condens. Matter* **24** 245401
[21] Evangelou S N and Pichard J L 2000 *Phys. Rev. Lett.* **84** 1643
[22] Ng G S and Kottos T 2007 *Phys. Rev. B* **75** 205120
[23] Ketzmerick R, Kruse K, Kraut S and Geisel T 1997 *Phys. Rev. Lett.* **79** 1959
[24] Zhong J, Diener R B, Steck D A, Oskay W H, Raizen M G, Plummer E W, Zhang Z and Niu Q 2001 *Phys. Rev. Lett.* **86** 2485
[25] Fermi E, Pasta J and Ulam S 1955 *Los Alamos report LA*-1940 (reprinted in *Collected Papers of Enrico Fermi*, Segre E ed., Vol. II, 1965, University of Chicago Press, p. 978)
[26] Berman G P and Izrailev F M 2005 *Chaos* **15** 015104
[27] Ovchinnikov A A, Erikhman N S and Pronin K A 2001 *Vibrational-Rotational Excitations in Nonlinear Molecular Systems* (New York: Kluwer Acedemic/Plenum Publishers) p. 298
[28] Zwanzig R 1960 *Lect. Theor. Phys.* **3** 106
[29] Benderskii V A, Falkovsky L A and Kats E I 2007 *JETP Lett.* **86** 221
[30] Likhachev V N, Astakhova T Y and Vinogradov G A 2014 *Theor. Math. Physics* **180** 1086
[31] Benderskii V A, Kotkin A S, Rubtsov I V and Kats E I 2013 *JETP Lett.* **98** 219
[32] Benderskii V A and Kats E I 2011 *JETP Lett.* **94** 459
[33] Ndawana M L, Römer R A and Schreiber M 2002 *Eur. Phys. J. B* **27** 399
[34] Deych L I, Lisyansky A A and Altshuler B L 2001 *Phys. Rev. B* **64** 224202
[35] MacKinnon A and Kramer B 1983 *Z. Phys. B-Condens. Matter* **53** 1
[36] MacKinnon A 1994 *J. Phys.: Condens. Matter* **6** 2511
[37] Pichard J L and Sarma G 1981 *J. Phys. C: Solid State Phys.* **14** L127
[38] Pichard J L and Sarma G 1981 *J. Phys. C: Solid State Phys.* **14** L617
[39] Elias B, Genereux J C and Barton J K 2008 *Angew. Chem. Int. Ed.* **47** 9067
[40] Gradstein I S and Ryzhik I M 2007 *Table of Integrals, Series, and Products* (7th edn.) (Amsterdam: Elsevier)
[41] Hufnagel L, Ketzmerick R, Kottos T and Geisel T 2001 *Phys. Rev. E* **64** 012301
[42] Zhang Z, Tong P, Gong J and Li B 2012 *Phys. Rev. Lett.* **108** 070603
[43] Conwell E M and Rakhmanova S V 2000 *Proc. Natl. Acad. Sci. USA* **97** 4556
[44] Rakhmanova S V and Conwell E M 2001 *J. Phys. Chem. B* **105** 2056
[45] Conwell E M and Basko D M 2001 *J. Am. Chem. Soc.* **123** 11441
[46] Conwell E M, Park J H and Choi H Y 2005 *J. Phys. Chem. B* **109** 9760
[47] Conwell E M, McLaughlin P M and Bloch S M 2008 *J. Phys. Chem. B* **112** 2268
[48] Zhang G, Hu H, Cui S and Lv Z 2010 *Physica B* **405** 4382
[49] Zhang G, Cui P, Wu J and Liu C 2009 *Physica B* **404** 1485
[50] Wei J H, Liu X J, Berakdar J and Yan Y 2008 *J. Chem. Phys.* **128** 165101
[51] Chakrabarti B, Piette B M A G and Zakrzewski W J 2012 *EPL* **97** 47005